Metasurfaces supporting topological states for efficient wave localization at GHz frequencies

A. D. Rozenblit, *Student Member, IEEE*, N. A. Olekhno, *Member, IEEE*

***Abstract*—Topological edge states of electromagnetic waves open new opportunities for designing photonic devices robust towards unavoidable manufacturing defects. The current paper presents the numerical simulations of the electrical circuit corresponding to the extended two-dimensional (2D) Su-Schrieffer-Heeger (SSH) model which supports an in-gap topological corner state at GHz frequencies. The results of the work highlight an essential role of the next-nearest couplings between the circuit sites for the emergence of topological states.**

I. Introduction

Topological edge states are eigenmodes featuring localization of the energy on the edges of the structure whose existence is governed by the symmetries of the bulk. Topological edge states have been realized with waves of different nature ranging from radiofrequency [1] and optical [2] systems to mechanical metamaterials [3]. Electrical circuits appear one of the platforms allowing to implement topological edge states. For instance, passive electrical circuits [4], circuits with operational amplifiers [5] and non-linear elements [6], and circuits working at the GHz frequencies [7] were used for demonstrating of topological states. Realization of the topological states in electrical circuits is based on the rigorous mathematical equivalence between the tight-binding equations and Kirchhoff's rules describing currents in the circuit.

II. Description of the Project

Recently, topological corner states located in the bandgap were experimentally demonstrated in the array of coupled microwave resonators realizing 2D SSH model [8, 9]. However, according to the theoretical predictions such a model supports a topological corner state in the continuum. To resolve this contradiction, we consider an extended 2D SSH model which differs from the conventional one by the newly introduced couplings M between the diagonally opposite next-nearest sites (Fig. 1(a)) [10]. The theoretical calculations for the model with 9×9 sites and tunneling couplings J=1, K=M=4 predict topological corner state in the bandgap (Fig. 1(b)).

The considered model can be described by the tight-binding equations. For example, the equation for the site with coordinates (2,2) has the following form:

$$J(\beta_{23}+\beta_{32})+K(\beta_{12}+\beta_{21})+M\beta_{11}=\varepsilon\beta_{22}, \qquad (1)$$

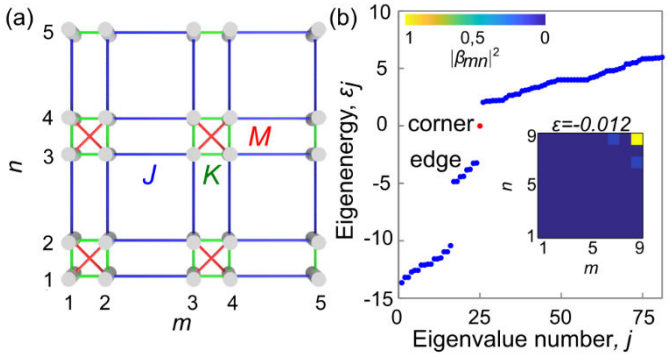

Fig. 1. (a) The schematic of the extended 2D SSH model with tunneling couplings J and K ($0<J<K$), and additional couplings M. (b) Spectrum of eigenenergies ε_j versus eigenvalue number j for the model from panel (a) with 9×9 sites and couplings J=1, K=M=4. The inset shows the field profile of the topological corner state.

where β_{mn} is the amplitude of the electrical field in a site with coordinates (m,n) and ε is the eigenenergy.

Figure 2(a) depicts the schematic of the electrical circuits corresponding to the extended 2D SSH model. According to the Kirchhoff's rules, the sum of currents flowing in the node with coordinates (2,2) can be represented in the following form:

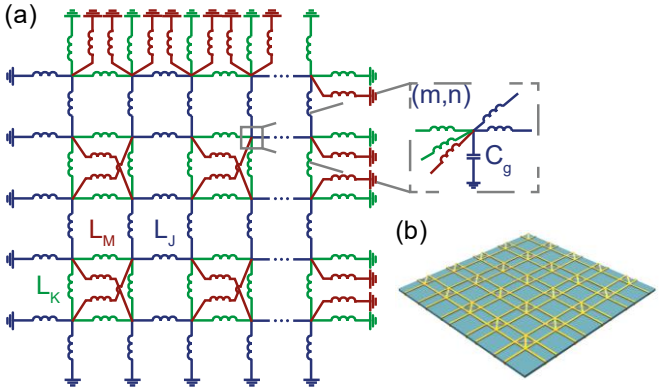

Fig. 2. (a) The schematic of the electrical circuit representing the extended 2D SSH model with inductance coils L_J, L_K, and L_M corresponding to the tunneling couplings J, K, and M, respectively. Each node is grounded by the capacitor C_g. (b) The microstrip metasurface design of the suggested electrical circuit with distributed parameters.

A.D. Rozenblit is a M.S. student at ITMO University, Saint Petersburg, Russia

N.A. Olekhno is a research fellow at ITMO University, Saint Petersburg, Russia

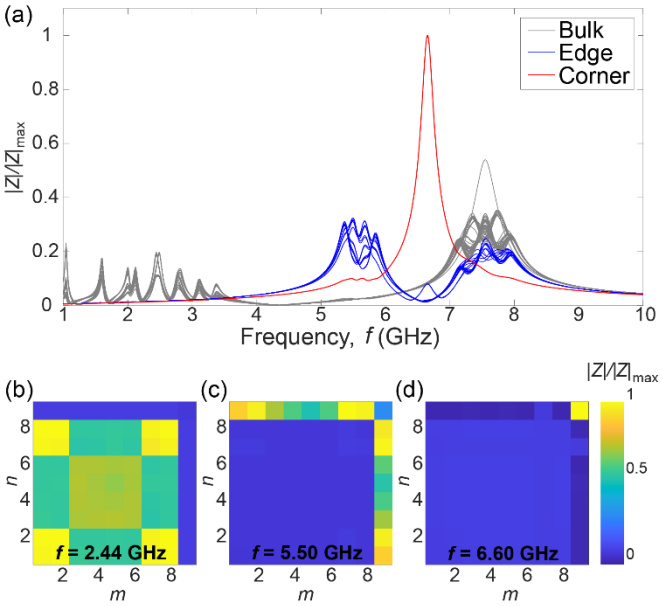

Fig. 3. (a) Normalized on-site impedance spectra for each node between the given node and ground. Gray curves correspond to the bulk nodes with coordinates ($1 \le m \le 8, 1 \le n \le 8$), blue ones – to the nodes with coordinates ($1 \le m \le 8, n=9$) and ($m=9, 1 \le n \le 8$), and red curve corresponds to the node (9,9). (b-d) Impedance distribution maps at frequencies of the bulk (b), topological edge (c), and topological corner (d) states.

$$-\sigma_{L_J}(\varphi_{23}+\varphi_{32}) - \sigma_{L_K}(\varphi_{12}+\varphi_{21}) - \sigma_{L_M}\varphi_{11} = \\ = -\left(2\sigma_{L_J} + 2\sigma_{L_K} + \sigma_{L_M} + \sigma_{C_g}\right)\varphi_{22}, \quad (2)$$

where σ_L and σ_C are admittances of links with inductors or capacitors respectively, and φ_{mn} is the electric potential at node with coordinates (n,m).

As seen, the equation for tight-binding model (1) and equation, describing currents in the circuit (2) are equivalent. Now, we can formulate the relation between the parameters of the tight-binding model and the parameters of the electrical circuit (for J=1):

$$K = \frac{L_J}{L_M}, M = \frac{L_J}{L_K}, \varepsilon = \frac{f^2}{f_0^2} - \left(2 + 2\frac{L_J}{L_K} + \frac{L_J}{L_M}\right), \quad (3)$$

where f is the resonant frequency and $f_0 = 1/(2\pi\sqrt{L_J C_g})$.

Using Keysight Advanced Design System software package, we performed numerical simulations of the impedance spectroscopy for each node of the circuit with size 9×9 nodes, L_J=4 (nH), L_K=L_M=1 (nH), and C_g=2 (pF). The normalized impedance spectra at frequency 1..10 GHz and impedance distribution maps at frequencies of the bulk, edge, and corner states are depicted in Figure 3. It is seen that, the topological corner state locates in the bandgap around 6.6 GHz.

III. Conclusion

We have demonstrated that the additional couplings between the diagonally-opposite sites in 2D SSH model lead to the emergence of the topological corner state in the bandgap. Numerical simulations of the resonances in the circuit corresponding to the extended 2D SSH model fully agree with theoretical predictions for the tight-binding model. Such circuits working at GHz frequencies can be implemented in the form of printed circuit boards with microstrips or lumped elements and used in a wide range of applications ranging from analog data processing to creating robust transmitters and receivers for Wi-Fi, LTE, or higher frequencies.

IV. Acknowledgments

The authors acknowledge fruitful discussions with Prof. Alexey Slobozhanyuk.

V. Award Impact and Future Plans

The IEEE MTT-S Undergraduate/Pregraduate Scholarship is one of the most prestigious awards in the field of microwave engineering for the students all over the world. For me, the award highlights the relevance of my scientific studies. The scholarship allowed me to stand out in the eyes both of other students as well as professors which might help me to attract collaborators in realization of my projects in future. Currently, I am finishing my Master's degree studies in Radiofrequency systems and devices program at ITMO University, Saint Petersburg, Russia. After the graduation, I plan to apply for a Ph.D. program at ITMO University and continue the research on microwaves focusing on industrial projects.

References

[1] M. Li, *et al*., "Higher-order topological states in photonic kagome crystals with long-range interactions," *Nature Photon*., vol. 14, pp. 89-94, Dec. 2020, doi: 10.1038/s41566-019-0561-9.

[2] A. Blanco-Redondo, *et al*., "Topological protection of biphoton states," *Science*, vol. 362, no. 6414, pp. 34-39, Nov. 2018, doi: 10.1126/scienceaau4296.

[3] R. Süsstrunk, et al., "Switchable topological phonon channels,", New J. Phys., vol. 19, pp. 015013, Jan. 2017, doi: 10.1088/1367-2630/aa591c.

[4] J. Ningyuan, *et al*., "Time- and Site-Resolved Dynamics in a Topological Circuit," *Phys. Rev. X*, vol. 5, pp. 021031, Jun. 2015, doi: 10.1103/PhysRevX.5.021031.

[5] S. Liu, *et al*., "Gain- and Loss-Induced Topological Insulating Phase in a Non-Hermitian Electrical Circuit," *Phys. Rev. Appl*., vol. 13, pp. 014047, Jan. 2020, doi: 10.1103/PhysRevApplied.13.014047.

[6] Y. Hadad, *et al*., "Self-induced topological protection in nonlinear circuit arrays", *Nat. Electron*., vol. 1, pp 178-182, Mar. 2018, doi: 10.1038/s41928-018-0042-z.

[7] Y. Li, *et al*., "Topological LC-circuits based on microstrips and observation of electromagnetic modes with orbital angular momentum," *Nat. Comm.* vol. 9, pp. 4598, Nov. 2018, doi: 10.1038/s41467-018-07084-2.

[8] X. Chen, *et al*., "Direct observation of corner states in second-order topological photonic crystal slabs," *Phys. Rev. Lett*., vol. 122, pp. 233902, Jun. 2019, doi: 10.1103/PhysRevLett.122.233902.

[9] B. Xie, *et al*., "Visualization of higher-order topological insulating phases in two-dimensional dielectric photonic crystals," *Phys. Rev. Lett*., vol. 122, pp. 233903, Jun. 2019, doi: 10.1103/PhysRevLett.122.233903.

[10] N. Olekhno, A. Rozenblit, *et al*., "Experimental realization of topological corner states in long-range-coupled electrical circuits," *Phys. Rev. B*, vol. 105, pp. L081107, Feb. 2022, doi: 10.1103/PhysRevB.105.L081107.